Experimental Pd II oscillator strengths and the palladium abundance in the HgMn-type star chi Lupi

Lundberg, Hans; Johansson, S. G; Larsson, Jörgen; Leckrone, D. S; Litzen, U; Svanberg, Sune; Wahlgren, G. M; Zerne, R

Published in:
Astrophysical Journal

DOI:
10.1086/177788

1996

THE ASTROPHYSICAL JOURNAL, 469:388–392, 1996 September 20

EXPERIMENTAL Pd II OSCILLATOR STRENGTHS AND THE PALLADIUM ABUNDANCE IN THE HgMn-TYPE STAR χ LUPI[1]

HANS LUNDBERG,[2] SVENERIC G. JOHANSSON,[3,4] JÖRGEN LARSSON,[2] DAVID S. LECKRONE,[5] ULF LITZÉN,[3] SUNE SVANBERG,[2] GLENN M. WAHLGREN,[3,6] AND RAOUL ZERNE[2]

Received 1996 January 17; accepted 1996 April 4

ABSTRACT

Experimental oscillator strengths for 19 ultraviolet lines of Pd II have been derived from measurements of line intensities in calibrated Fourier transform spectra, combined with picosecond-pulse laser measurements of radiative lifetimes. Five of these 19 lines, in addition to other Pd II lines, are present in *Hubble Space Telescope*/Goddard High-Resolution Spectrograph echelle spectra of the chemically peculiar HgMn star χ Lupi, yielding a palladium abundance of log $(N_{Pd}) = +5.0$, which is 3.3 dex above the solar abundance. Theoretical oscillator strengths have been calculated for all strong ultraviolet transitions associated with the lowest odd-parity configuration of Pd II.

Subject headings: atomic data — line: identification — stars: abundances — stars: individual (χ Lupi) — ultraviolet: stars

1. INTRODUCTION

In a previous paper Johansson et al. (1994) combined experimental and observational data to determine the abundance of ruthenium in the chemically peculiar (CP) HgMn-type star χ Lupi. The laboratory data included measurements of atomic lifetimes and branching fractions for some Ru II lines, from which absolute oscillator strengths were derived. These were applied to seven Ru II lines in the ultraviolet (UV) spectrum of χ Lupi, obtained with the Goddard High-Resolution Spectrograph (GHRS) on board the *Hubble Space Telescope* (*HST*). The agreement between observed and calculated line profiles using the new Ru II data was good and within the combined uncertainties. The same method has now been applied to five newly identified Pd II lines in the GHRS spectrum of χ Lupi. The identifications are based on coincidences between unidentified features in the stellar spectrum and strong laboratory lines of Pd II, recently remeasured by Lundberg, Litzén, & Johansson (1994). We identified 19 Pd II lines originating from the $4d^8 5p$ configuration in our GHRS spectra. The wavelength agreement between the laboratory lines and stellar features was typically 0.005 Å. Palladium is homologous to nickel, and the atomic structure of Pd II mimics that of Ni II. The ground term $4d^9\ ^2D$ lies more than 8 eV below the excited $4d^8 5p$ configuration, placing the resonance lines in the 1300–1400 Å region. The Pd II lines studied in this work appear at wavelengths longward of 2000 Å and result from $4d^8 5s$–$4d^8 5p$ transitions. Experimental oscillator strengths have been determined from measurements of branching fractions and radiative lifetimes. The branching fractions were obtained from line intensities in Fourier transform spectra, and the radiative lifetimes were measured in time-resolved laser experiments. The palladium abundance in the primary star of the multiple-star system χ Lupi was determined by fitting calculated line profiles to observed *HST* spectra. Theoretical oscillator strengths have been calculated for all strong transitions between the $4d^8 5p$ and $4d^8 5s$ configurations in Pd II.

2. WAVELENGTHS AND BRANCHING FRACTIONS

In an earlier work wavelengths and line intensities for Pd II were measured in the wavelength region 1900–5000 Å using Fourier transform spectroscopy (Lundberg et al. 1994). Many Pd II lines in this region are due to transitions between the low configurations $4d^8 5s$ and $4d^8 5p$. In that work a hollow cathode discharge was used as a light source, and the accuracy of the wavelength determinations was approximately 1 mÅ. In addition to the measurements of wavelength and peak intensity, Voigt functions were fitted to the observed line profiles, and the area under the fitted curve was adopted as a measure of the intensity. Direct measurements of oscillator strengths require absolute values for the observed intensity. This approach, in turn, requires knowledge of certain light-source parameters and the absolute efficiency of the spectrometer and detector. In most experimental situations it is difficult to obtain this information accurately. A more versatile method, used in this work, is to measure relative intensities or branching fractions and then perform a normalization using an experimental lifetime. When using this method, however, relative intensities for all lines with a common upper level must be known. This can be cumbersome if the lines are spread over long wavelength intervals and different types of recording equipment are used. In the present work Einstein *A*-values were obtained for lines originating from four levels belonging to the $4d^8 5p$ configuration with energies of 70,000 to 80,000 cm^{-1}. These levels decay to states of the $4d^8 5s$ configuration through lines, most of which appear in the recorded wavelength region. However, three of the levels

[1] Based on observations with the NASA/ESA *Hubble Space Telescope*, obtained at the Space Telescope Science Institute, which is operated by the Association of Universities for Research in Astronomy, Inc., under NASA contract NASA-26555.

[2] Department of Physics, Lund Institute of Technology, Box 118, S-22100, Lund, Sweden.

[3] Department of Physics, Lund University, Sölvegatan 14, S-22362 Lund, Sweden.

[4] Lund Observatory, Lund University, Box 43, S-22100 Lund, Sweden.

[5] Laboratory for Astronomy and Solar Physics, NASA/Goddard Space Flight Center, Code 681, Greenbelt, MD, 20771.

[6] Astronomy Programs, Computer Sciences Corporation and GHRS Science Team, NASA/Goddard Space Flight Center, Code 681, Greenbelt, MD 20771.

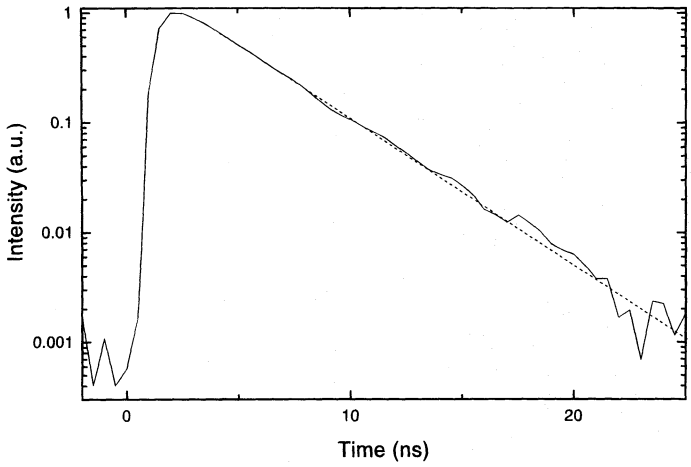

FIG. 1.—A fluorescence decay curve for the Pd II level at 69,881.712 cm^{-1}. Plasma background light has been subtracted. The decay, following the pulsed excitation, was captured by a microchannel plate photomultiplier tube connected to a digital oscilloscope.

have branches to the ground state at shorter wavelengths, and calculated A-values were used to account for these transitions. To obtain branching fractions from the recorded intensities, the wavelength dependent efficiency of the spectrometer system must be obtained. It is an advantage if this can be done using reference lines present in the spectra to be calibrated. In the Pd II recordings, either an Ar or an He-Ne mixture was used as the carrier gas, and the efficiency function was obtained from known branching ratios of Ar II lines (Whaling, Carle, & Pitt 1993). However, the branching fractions for Pd II were evaluated utilizing the He-Ne recordings because of a stronger population of the high energy levels in such a discharge. In that procedure we applied the efficiency function obtained using the Ar-Pd hollow cathode. For the theoretical calculations, knowledge of the $4d^7 5s5p$ configuration is important because of its interaction with the $4d^8 5p$ levels (see § 4). Pd II wavelengths in the region 1000–1900 Å were derived from photographic plate data obtained with the 10 m spectrograph at the Observatoire de Paris, Meudon. These wavelengths enabled an analysis of the positions of the lowest energy levels of the $4d^7 5s5p$ configuration, which were included in the calculations. The analysis of this configuration will be published elsewhere.

3. RADIATIVE LIFETIMES

Radiative lifetimes were measured for four levels belonging to the $4d^8 5p$ configuration. In the experiments free palladium ions were created in a laser-produced plasma. A rotating palladium target was irradiated with a neodymium-doped yttrium aluminum garnet (Nd:YAG) laser, giving pulses with 10 ns duration. The pulses had an energy of about 25 mJ and were focused onto the target by a 30 cm focal length lens. Metastable levels belonging to the $4d^8 5s$ configuration and with an energy around 25,000 cm^{-1} were then populated in the plasma. Ions were selectively photoexcited from one of these levels to the state under investigation by the light from a dye laser. In order to obtain short duration pulses a distributed feedback dye laser (DFDL) was used. It provided 70 ps duration pulses, which are much shorter than the measured lifetimes. Laser-produced plasmas have been used frequently to produce free atoms or ions of elements with high melting points. It has been found that the plasma environment does not present a problem for accurate determinations of lifetimes of the order of a few nanoseconds (Bergström et al. 1988). For free atoms or ions in the ground state the laser beam can interact with the ions located rather far from the target and for comparatively long periods of time after the plasma has been produced, e.g., in the afterglow of the plasma. In these measurements, however, the optical excitation

TABLE 1

PD II ATOMIC DATA AND DERIVED ABUNDANCES

Level Data (cm^{-1})	Line (Å)	Einstein A (10^8 s^{-1})	log gf (Experiment)	log gf (Theory)	log (N_{Pd})
69881.712	2658.7201	0.37	−0.40	−0.24	...
$J = 9/2$	2336.5869	0.58	−0.32	−0.09	+6.05
$\tau_{exp} = 3.2 \pm 0.3$ ns.....	2331.5907	2.16	+0.21	+0.36	...
$\tau_{cal} = 2.2$ ns	...	...	...	...	...
73330.716	2698.5351	0.07	−1.24	−1.14	...
$J = 7/2$	2569.5444	0.43	−0.47	−0.37	...
$\tau_{exp} = 2.9 \pm 0.3$ ns.....	2435.3210	1.63	+0.06	+0.24	+5.05
$\tau_{cal} = 2.1$ ns	2251.5028	0.30	−0.73	−0.66	...
... .	2162.2617	0.54	−0.52	−0.47	...
... .	2072.0423	0.08	−1.39	−1.23	...
... .	1363.685	0.44	−1.00	−0.86	...
74321.488	2628.2406	0.47	−0.41	−0.34	...
$J = 7/2$	2505.7293	1.61	+0.08	+0.19	...
$\tau_{exp} = 2.6 \pm 0.3$ ns.....	2377.9234	0.22	−0.82	−0.74	+5.15
$\tau_{cal} = 2.1$ ns	2202.3542	0.99	−0.24	−0.15	+5.10
... .	2116.8917	0.03	−1.88	−2.04	...
... .	1345.506	0.61	−0.87	−0.78	...
79711.296	2839.8790	0.05	−1.36	−1.08	...
$J = 7/2$	2595.9563	0.49	−0.40	−0.72	...
$\tau_{exp} = 1.5 \pm 0.3$ ns.....	2302.0204	3.73	+0.37	+0.29	...
$\tau_{cal} = 1.8$ ns	2207.4835	1.30	−0.12	−0.20	+4.80
... .	2107.6811	0.04	−1.66	−1.77	...
... .	1254.527	0.97	−0.74	−0.82	...

occurred from comparatively high metastable levels, and in order to have a substantial population of these levels, it was necessary to have a short delay between the creation of the plasma and the dye laser pulse. The plasma expands rapidly, and the density is much higher at early stages of its evolution. Collisions can then cause a shortening of recorded lifetimes. In the measurements the delay was increased until no systematic change in the lifetime was observed. A delay of 0.4 μs was sufficient for the highest metastable level, whereas the population was too low after 0.6 μs. These numbers correspond to a laser excitation located 5 mm from the target. The dye laser was pumped by a mode-locked and Q-switched Nd:YAG laser. The dye laser output, tunable in the region 7000–8000 Å, was amplified to a pulse energy of about 1 mJ. The laser pulses were mixed with the fourth harmonic of the Nd:YAG laser in a crystal giving the desired excitation wavelengths between 2000 and 2200 Å. The bandwidth of the laser light was about 0.3 Å. Fluorescence light was detected in a direction perpendicular to the flight direction of the ions and the direction of the exciting radiation. One decay channel, different from the excitation, was selected using a 0.25 m monochromator, which also reduced the continuous background radiation from the plasma. The decay was recorded by a microchannel plate photomultiplier tube connected to a digital oscilloscope. For each lifetime measurement three recordings were made: the dye laser pulse without plasma, the plasma background light without dye laser, and the fluorescence decay. In the evaluation procedure the second curve was subtracted from the third in order to subtract plasma background. Figure 1 shows a decay curve obtained in this way. To avoid possible effects due to the limited time resolution in the detection system, the lifetime value was finally obtained by a least-squares fit to a convolution of the recorded laser pulse and an exponential curve. The lifetime values are given in Table 1.

4. OSCILLATOR STRENGTHS

Theoretical oscillator strengths were obtained using the Cowan computer code package (Cowan 1981; Ralchenko & Kramida 1995). The final calculations were performed using wave functions obtained after a least-squares fit of calculated levels to observed energy levels. The configurations $4d^9$, $4d^85s$, $4d^86s$, $4d^85d$, $4d^75s^2$, $4d^85p$, and $4d^75s5p$ were included in the calculations. The log *gf*-values were calculated for all transitions between the $4d^85p$ and $4d^85s$ configurations that were observed by Lundberg et al. (1994), and a complete list is available upon request. In Table 1 we only include values for those transitions that were investigated experimentally. The four levels, for which lifetimes were measured, were chosen because lines that were observed in *HST* spectra originate from these levels. The level $J = 9/2$ does not combine with the ground state, and all lines from this level were covered by the Fourier transform spectra. For the other levels the branching fractions to the ground state were taken from the Cowan calculations. The highest level has transitions to the $4d^85s$ configuration at wavelengths below 1900 Å as well as possible unknown infrared transitions to the $4d^75s^2$ configuration. According to the calculations, the former contribute 5% to the total decay, whereas the latter are negligible. Other transitions to the $4d^85s$ configuration were calculated to be at least 1 order of magnitude weaker than any of those listed, and they were not detected in the Fourier transform spectra. The experimental lifetimes given in the first column of Table 1 have error bars set by the statistical spread amongst the different recordings. For the lifetimes it can be seen that the calculated values have a rather small spread around 2 ns, while the experimental value differs by more than a factor of 2. For other levels in the configuration, however, the Cowan calculations show a larger variation. In the fifth column the calculated log *gf*-values are given for comparison. The table also includes three transitions to the ground state although these lines appear at shorter wavelengths and thus were not observed in the intensity-calibrated spectra. The values reported as experimental are in these cases equal to the theoretical values rescaled by means of the experimental lifetime. As already mentioned, in the evaluation of experimental log *gf*-values the relative intensities were taken from the recordings using He-Ne as a carrier gas. An estimate of the errors in the branching fractions due to noise in the recorded profiles can be obtained by comparing with results from the argon recordings or using peak intensities instead of areas under fitted curves. This procedure shows a variation of typically 20%. The relative error in the lifetimes is 10%–20%. To this, one should add an uncertainty in the efficiency calibration. Three of the four levels have branches in unobserved lines. These were taken from the calculations and correspond to 15%–20% of the total decay. The intensities of the Pd II lines are much higher in the He-Ne than in the Ar recordings, indicating a considerably lower Pd^+ density in the latter case. Comparisons between line ratios from the two recordings indicate that the influence from self-absorption on the branching fractions is negligible compared to the other sources of error. In total, an estimated uncertainty of 40% corresponds to ± 0.15 dex in the log *gf*-value.

5. ASTROPHYSICAL APPLICATIONS

Use of the GHRS echelle mode together with the experimental results discussed in the previous sections have allowed us to identify and analyze Pd II lines found in the UV spectrum of the CP HgMn-type primary star of the χ Lupi (B9.5p HgMn + A2Vm) binary star system. CP stars are known to exhibit strong spectral lines from a variety of heavy elements. Among the stars of the CP magnetic sequence (Ap stars), spectral lines of Pd I have been identified in optical region spectrograms of γ Equ (Adelman, Bidelman, & Pyper 1979) and HR 465 (Bidelman 1966; Bidelman, Cowley, & Iler 1995; Cowley et al. 1973; Hartoog, Cowley, & Cowley 1973). For HR 465 Cowley et al. (1973) determined the abundance log $N_{Pd} = +6.4$ from three Pd I lines (on a scale where log H = 12.00). A Pd I abundance has also been estimated for the Sun, +1.69 (Biemont et al. 1982), and Procyon, +1.60 (Orlov & Shavrina 1991). We refer the interested reader to the recent work of Jaschek & Jaschek (1995) for discussions pertaining to elemental identifications in stellar spectra. χ Lupi has been the subject of both optical and UV studies as a result of its extremely sharp spectral lines that originate from its low rotational velocity and small atmospheric turbulent mixing. Its UV spectrum is an excellent resource for researching problems in atomic physics under physical conditions that are not normally found in the laboratory (Johansson et al. 1995) or that originate from elements/ions that exist at trace abundance levels in stars of more solar-like chemical composition. The GHRS spectra used in this study were obtained during 1993 February as part of *HST* GTO

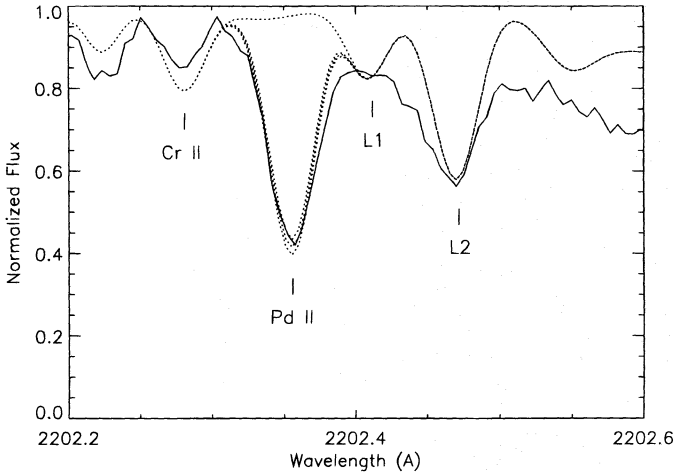

FIG. 2.—Pd II λ2202.354 in χ Lupi. The observation ($\Delta\lambda = +0.358$, LR = 6.22, R = 93,470) is compared with calculations for the abundances log (N_{Pd}) = 1.70, 5.0, 5.1, and 5.2. Two lines, L1 and L2, have been introduced into the line list for the purpose of additional line opacity, but with negligible effect upon the Pd II line profile.

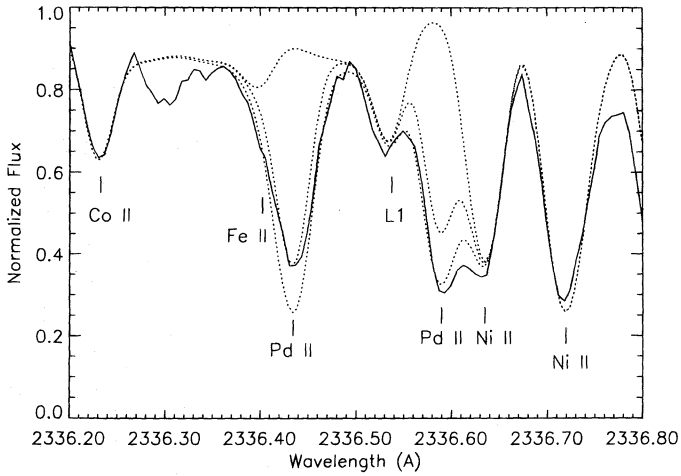

FIG. 4.—Pd II λ2336.587 in χ Lupi. The observation ($\Delta\lambda = +0.362$, LR = 6.06, R = 85,820) is compared with calculations for the abundances log (N_{Pd}) = 1.70, 5.1, and 6.0. The fake line L1 has been added for opacity purposes. The Pd II λ2336.435, for which we have a calculated *gf*-value, is well fitted in depth by the 5.1 abundance, but is obviously incorrect when using the 6.0 abundance, derived from the "best-fit single-line" scenario of the λ2336.587 line.

proposal 3961. The data reduction and synthetic spectrum analysis techniques employed have been discussed by Leckrone et al. (1993) and Wahlgren et al. (1995). The data typically have signal-to-noise ratios between 60 and 80 at the continuum level. The GHRS echelle mode provides spectral resolving powers between $R = \delta\lambda/\lambda$ = 80,000 and 95,000. Each of the four observations that were employed in this analysis was independently normalized by a technique that utilizes synthetic spectra to identify the actual continuum level, which often occurs at higher flux values than are found the spectrum peaks. The palladium abundance in the primary star χ Lupi A was determined by fitting the flux normalized observations with spectra generated by the program SYNTHE (Kurucz & Avrett 1981), using ATLAS8 model atmospheres created from the stellar parameters determined by Wahlgren, Adelman, & Robinson (1994). The co-addition of spectra generated for each of the binary star components was based upon the ephemeris of Dworetsky (1972). Five of the lines presented in Table 1 are located within the bounds of the spectral data obtained to date for χ Lupi. Additional lines of Pd II have also been identified in the data; however, without accurate *gf*-values these lines take on a supportive role in the abundance determination. Lines of Pd II were not identified in the secondary star spectrum. Although terrestrial palladium is composed of six isotopes, we do not see any structure or asymmetry in the laboratory line profiles. Thus, there is no measurable effect upon the positions and shapes of line profiles either in our laboratory spectra or in the stellar spectra, and we have modeled the stellar Pd II lines as single-component structures. The bulk of the atomic line data in the synthetic spectrum calculations are taken from the compilations of Kurucz (1991). Figures 2 through 6 illustrate the results of the synthetic spectrum analysis. Each of the figure captions

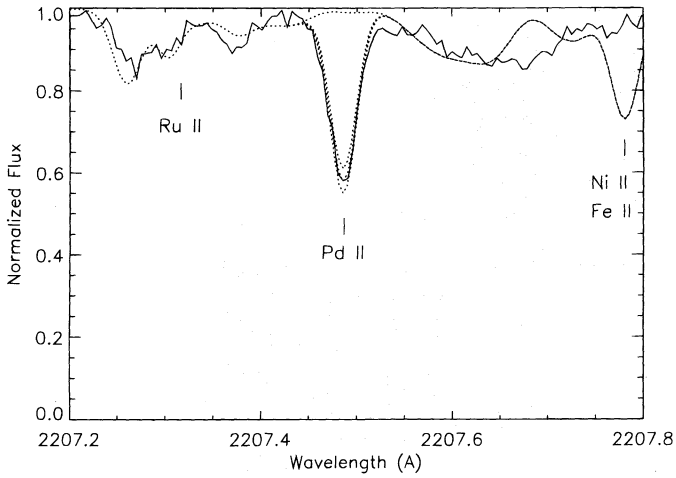

FIG. 3.—Pd II λ2207.484 in χ Lupi. The observation ($\Delta\lambda = +0.358$, LR = 6.22, R = 93,470) is compared with calculations for the abundances log (N_{Pd}) = 1.70, 4.65, 4.75, and 4.85. For Ru II λ2207.302 the laboratory-determined *gf*-value of 0.036 produces a good fit to the observation with an abundance of log (N_{Ru}) = 4.1 (Johansson et al. 1994).

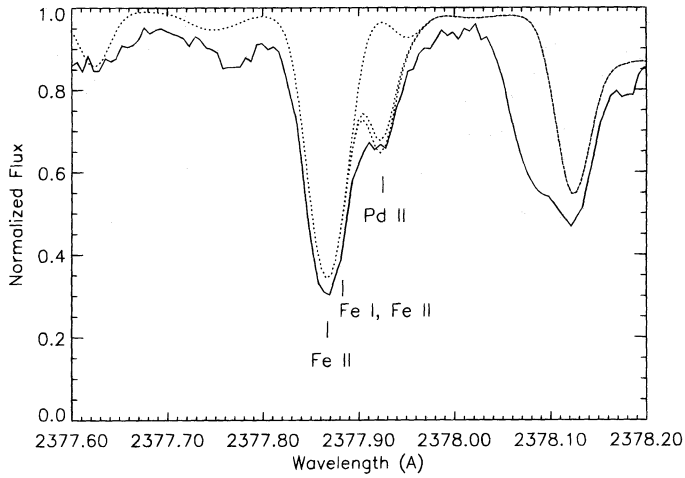

FIG. 5.—Pd II λ2377.923 in χ Lupi. The observation ($\Delta\lambda = +0.366$, LR = 6.02, R = 92,140) is compared with calculations for the abundances log (N_{Pd}) = 1.70, 5.1, and 5.2.

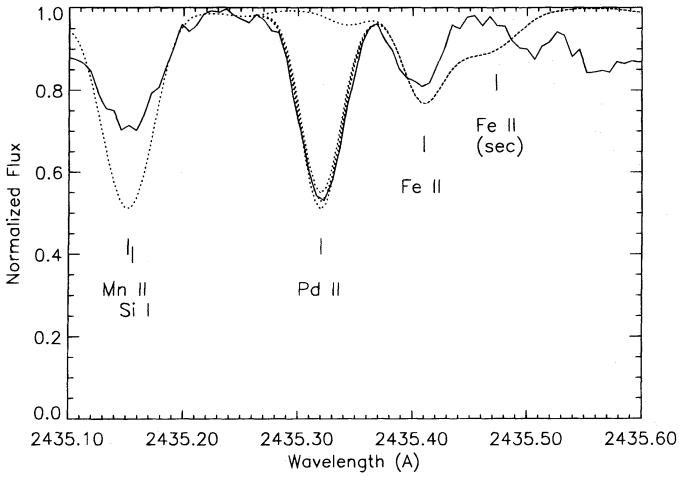

FIG. 6.—Pd II λ2435.321 in χ Lupi. The observation ($\Delta\lambda = +0.361$, LR = 5.95, R = 85,550) is compared with calculations for the abundances log (N_{Pd}) = 1.70, 4.9, 5.0, and 5.1. The poor fit to the Mn II + Si I feature is not the result of improper abundances, but is likely to result from incorrect oscillator strength(s).

lists the following: the wavelength separation, $\Delta\lambda = \lambda_{primary} - \lambda_{secondary}$, between spectra of the binary system components at the observation epoch; the light ratio, LR = $L_{primary}/L_{secondary}$, used in the co-addition process; and the resolving power, R, for the observation. In each of the figures the observation (*solid line*) is compared with calculations (*dotted lines*) representing several values of the palladium abundance, including the solar value of log (N_{Pd}) = 1.7. In all cases the data have not been smoothed. Three of the lines, Pd II $\lambda\lambda$2202.354, 2207.484, and 2435.321 are relatively isolated, while the lines located at $\lambda\lambda$2336.587 and 2377.923 are components of more blended spectral features. We have introduced fictitious atomic lines into the analysis of the Pd II $\lambda\lambda$2202.354 and 2336.587 features as sources of blending opacity. However, their effect upon Pd II line profiles is minimal. We suspect that the Pd II abundance derived from the λ2336.587 line is unrealistically high as a result of the presence of an unidentified spectral line(s), and we therefore exclude it from the final Pd II abundance value quoted. The other lines provide reasonably consistent results and no evidence for the exclusion of additional lines from the Pd II abundance determination. A straight averaging of the derived abundances from the remaining four lines, as presented in Table 1, yields log (N_{Pd}) = +5.0. Figure 4 also includes the line Pd II λ2336.432, for which we have obtained $gf = +1.156$ from a Cowan code calculation. Its depth is matched well by the average Pd abundance determined, but its greater observed width indicates that other blending lines, for which we have no knowledge at the present time, are likely to be present. Thus, the abundance of palladium in χ Lupi is determined to be 3.3 dex greater than the solar value. However, we caution the reader that comparisons of elemental abundances made between HgMn stars and the Sun may be affected by the choice of ion and our understanding of the physical mechanisms that are responsible for the great line strengths in HgMn stars. The enhancement of palladium is approximately 1.5 orders of magnitude greater than the Ru II enhancement in χ Lupi (Johansson et al. 1994) and nearly 3 orders of magnitude greater than the Cd II enhancement (Wahlgren et al. 1995). Lines from the adjacent odd atomic number elements Rh and Ag have yet to be detected. In χ Lupi, the palladium abundance enhancement is only surpassed by those for the very heavy ions platinum, gold, and mercury (Wahlgren et al. 1995) and thallium (Leckrone et al. 1996).

This work was supported by the Swedish Natural Science Research Council and the Swedish National Space Board. G. M. W. also gratefully acknowledges financial support received from NORDITA and the Swedish National Science Research Council (NFR). The authors also thank the referee, C. Cowley, for his valuable comments.

REFERENCES

Adelman, S. J., Bidelman, W. P., & Pyper, D. M. 1979, ApJS, 40, 371
Bergström, H., Faris, G. W., Hallstadius, H., Lundberg, H., Persson, A., & Wahlström, C. -G. 1988, Z. Phys., D8, 17
Bidelman, W. P. 1966, in IAU Symp. 26, Abundance Determinations in Stellar Spectra, ed. H. Hubenet (London: Academic), 229
Bidelman, W. P., Cowley, C. R., & Iler, A. L. 1995, Pub. Obs. Univ. Michigan, 12, No. 3
Biemont, E., Grevesse, N., Kwiatkowski, M., & Zimmerman, P. 1982, A&A, 108, 127
Cowan, R. D. 1981, The Theory of Atomic Structure and Spectra (Berkeley: Univ. of California Press)
Cowley, C. R., Hartoog, M. R., Aller, M. E., & Cowley, A. P. 1973, ApJ, 183, 127
Dworetsky, M. M. 1972, PASP, 84, 254
Hartoog, M. R., Cowley, C. R., & Cowley, A. P. 1973, ApJ, 182, 847
Jaschek, C., & Jaschek, M. 1995, The Behavior of the Chemical Elements in Stars (Cambridge: Cambridge Univ. Press)
Johansson, S., Brage, T., Leckrone, D. S., Nave, G., & Wahlgren, G. M. 1995, ApJ, 446, 361
Johansson, S. E., Joueizadeh, A., Litzén, U., Larsson, J., Persson, A., Wahlstrom, C.-G., Svanberg, S., Leckrone, D. S., & Wahlgren, G. M. 1994, ApJ, 421, 809
Kurucz, R. L. 1991, in Stellar Atmospheres: Beyond Classical Methods, ed. L. Crivellari, I. Hubeny, & D. G. Hummer (Dordrecht : Kluwer), 441
Kurucz, R. L., & Avrett, E. H. 1981, SAO Special Rep. 391
Leckrone, D. S., Johansson, S. G., Kalus, G., Wahlgren, G. M., Brage, T., & Profitt, C. R. 1996, ApJ, 462, 937
Leckrone, D. S., Johansson, S., Wahlgren, G. M., & Adelman, S. J. 1993, Phys. Scr., T47, 149
Lundberg, H., Litzén, U., & Johansson, S. 1994, Phys. Scr., 50, 110
Orlov, M. Ya., & Shavrina, A. V. 1991, Soviet Astron. Lett., 17, 227
Ralchenko, Yu. V., & Kramida, A. E. 1995, private communication
Wahlgren, G. M., Adelman, S. J., & Robinson, R. D. 1994, ApJ, 434, 349
Wahlgren, G. M., Leckrone, D. S., Johansson, S. G., Rosberg, M., & Brage, T. 1995, ApJ, 444, 438
Whaling, W., Carle, M. T., & Pitt, M. L. 1993, J. Quant. Spectrosc. Radiat. Transfer, 50, 7